MOLECULAR PHYSICS REPORTS **40** (2004) 150-155

NUMERICAL SIMULATIONS OF MAGNETIZATION DISTRIBUTION AND MAGNETIZATION PROCESSES IN ULTRATHIN FILMS

W. STEFANOWICZ, M. KISIELEWSKI, AND A. MAZIEWSKI

Laboratory of Magnetism, Institute of Experimental Physics
University of Białystok, 41 Lipowa str., 15-424 Białystok, Poland

Abstract: The evolution of magnetization distributions and magnetization processes in ultrathin films near the reorientation phase transition (RPT) from easy magnetization axis, perpendicular to the sample plane, into easy magnetization plane, was studied by simulations. Simulations were performed for material parameters found for ultrathin cobalt in a gold envelope. Sinusoidal-like distributions were obtained near the RPT. A decrease of both the oscillation amplitude and the initial susceptibility was found while approaching the RPT.

In recent years ultrathin ferromagnetic films have attracted a tremendous amount of attention. Although the magnetism of uniform bulk materials of micrometer sizes is well known and circumscribed [1], the magnetic order of ultrathin films, or samples of thickness of a few atomic layers, has many secrets inside.

A typical phenomenon observed in ultrathin magnetic films is the strong dependence of magnetic anisotropy on sample thickness d. This dependence is connected with strong thickness dependence of the surface anisotropy for small thickness (smaller than 2 nm) in relation to the volume anisotropy.

The purpose of this work is to find, by computer simulations, the magnetization distribution at different values of the perpendicularly-oriented magnetic field near the thickness-driven RPT.

The energy of the uniaxial magnetic anisotropy of an ultrathin film may be described by the well known equation:

$$E_A = K_{1\mathrm{eff}} \sin^2(\theta)$$

where $K_{1\mathrm{eff}} = K_{1V} + 2K_{1S}/d - 2\pi M_S$ and $K_{1\mathrm{eff}}$ is the effective anisotropy constant, K_{1V} – the volume anisotropy constant, K_{1S} – the mean surface anisotropy constant, M_S – saturation magnetization, and θ – the angle between the magnetization vector and normal to the sample plane. This thickness dependence of the anisotropy leads to the change of the sign of $K_{1\mathrm{eff}}$ from positive to negative, with an increase of sample thickness d (Fig. 1). The RPT is defined by the critical thickness d_1, in which $K_{1\mathrm{eff}}(d_1) = 0$. The magnetization vector changes orientation from perpendicular to the plane of the sample one ("out-of-plane" phase) to the parallel one ("in-plane" phase).

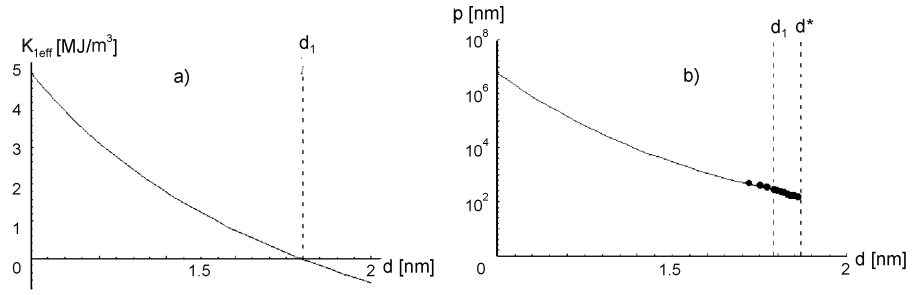

Fig. 1. The thickness dependence of: a) the effective anisotropy constant $K_{1\text{eff}}$ [4], b) the period of domain structure. Solid curve was fitted to results obtained in Ref. [2], points were obtained from simulations

Stripe domain structure as a function of sample thickness d is considered. Outside the RPT, domain period p is much larger than domain wall width δ_w. Approaching the RPT the domain structure transforms into a sinusoidal one up to $p^*(d^*)$ [2], and period p drastically decreases. By increasing d, the strong p decrease was determined by SEMPA techniques [3].

Let us consider the magnetization process in the monodomain state. The total energy of the sample consists of the Zeeman energy and the energy of the magnetic anisotropy:

$$E_{\text{tot}} = -HM - 2\pi M_S^2 Q_{\text{1eff}} \sin^2(\theta) \tag{1}$$

where $Q_{\text{1eff}} = K_{\text{1eff}} / 2\pi M_S^2$ is the effective quality factor. Substituting the following normalized values $m = M/M_S$, $h = H/4\pi M_S$, and minimizing the total energy in respect to the angle θ, we have found the following terms: $\cos(\theta) = -h/Q_{\text{1eff}} \left(= m_\perp\right)$ and:

$$\chi_\perp = -1/4\pi Q_{\text{1eff}} \tag{2}$$

The $\chi_\perp(d)$ curve is drawn in Fig. 2 by a solid line, considering the $K_{1\text{eff}}(d)$ dependence [4].

This magnetization distribution study was supported by OOMMF (Objective Oriented MicroMagnetic Framework) software [5]. Simulations were made near the RPT by minimization of the total energy of the rectangular sample with geometry shown in Fig. 3. For simulations, the magnetic parameters found for Au/Co/Au ultrathin films [4] with d_1=1.79 nm and d^*=1.868 nm were taken.

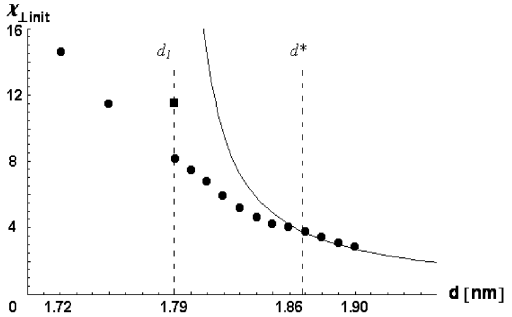

Fig. 2. Dependence of the initial susceptibility on sample thickness: calculated (points) and theoretical (solid line)

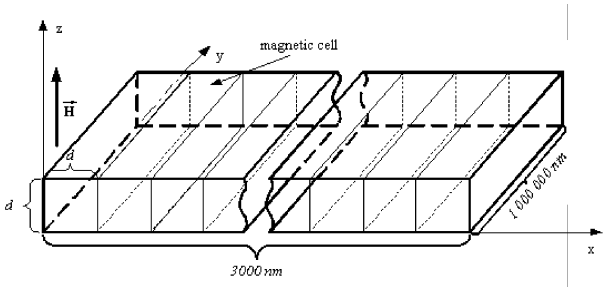

Fig. 3. Geometry of the simulated sample

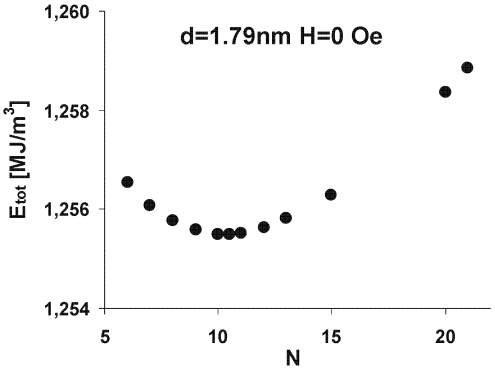

Fig. 4. Dependence of the total energy on N – the number of domain structure periods, calculated for a sample with thickness d_1 in a zero magnetic field

Simulations were usually started with sinusoidal-like magnetization distribution characterized by period p or N – number of periods in the sample. Any final magnetization distribution was characterized by the total energy E_{tot} and the number of periods, which was usually equal to N – the starting number. Figure 4 shows an example of $E_{tot}(N)$ obtained for a 1.79 nm thick sample without any external magnetic field. Simulated magnetization distribution with minimal E_{tot} was chosen for the next step of analysis. Insets "a" ($H_\perp = 0$) to Figs. 6-8 show magnetic anisotropy-induced changes of these zero-field distributions. Magnetization oscillation amplitude decreases while lowering Q_{1eff}. One can calculate the average normal magnetization component $<m_\perp(x)>$. However, the geometry of a finite sample with boundary has influence on the calculated $<m_\perp(x)>$ value. This is illustrated in Fig. 5 where $<m_\perp(x)>$ values were calculated for a different averaging range, measured in the number of domain periods N_{av}. The range was taken from the sample center. Performing whole sample averaging, one can find a nonzero mean $<m_\perp(x)>$ value for $d = 1.86$ without an external field, see Fig. 5b. The boundary effect influence could be limited by decreasing the $<m_\perp(x)>$ averaging range. This is important for determining susceptibility. Initial susceptibility was calculated using $<m_\perp(x)>$ (H) values. Figure 2 shows $\chi_{\perp init}$ marked by full circles, where $<m_\perp(x)>$ was determined from a limited range; the full square denotes $\chi_{\perp init}$ calculated for $d = 1.79$ nm with $<m_\perp(x)>$ averaging for the whole sample.

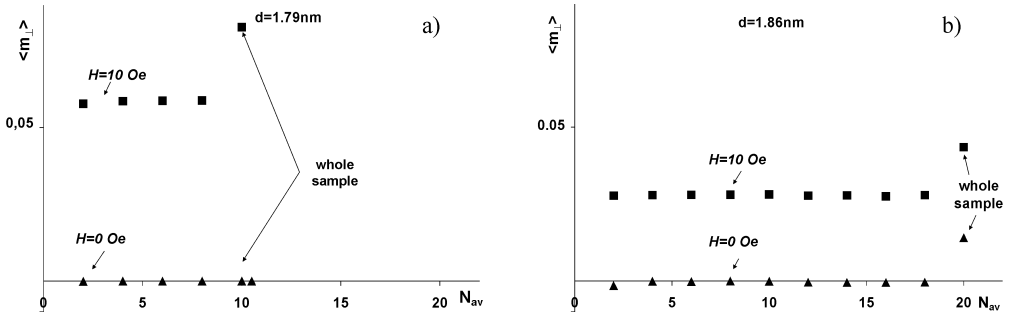

Fig. 5. Dependence of mean magnetization $<m_\perp(x)>$ on averaging range, measured in number of periods N_{av}, determined for sample thickness: a) d = 1.79 nm and b) d = 1.86 nm

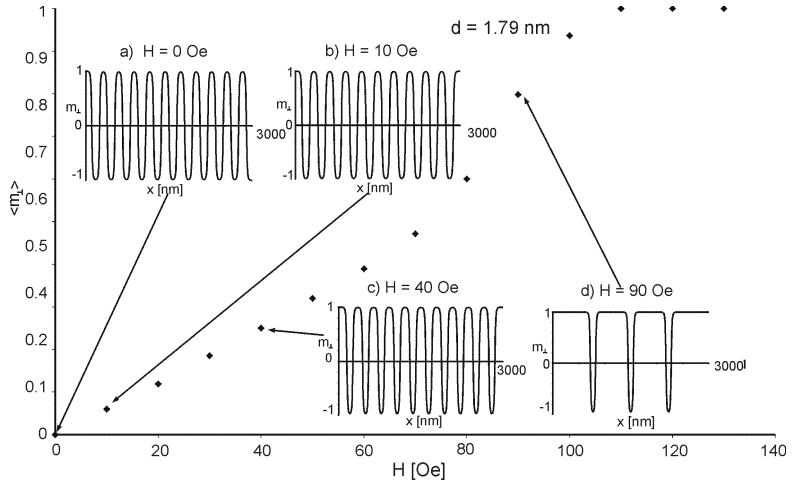

Fig. 6. Dependence of the average $<m_\perp>$ magnetization component on an external field, for d = 1.79 nm. Insets a)-d) show $m_\perp(x)$ magnetization component distributions for points indicated by arrows

Now, let us consider magnetization processes for three selected thicknesses.

Figure 6 shows results obtained for the sample with $d = d_1 = 1.79$ nm. In a zero magnetic field, magnetization distribution is sinusoidal-like with an amplitude equal to one. In external magnetic field H = 10 Oe, one can see not only changes of domain structure but changes of the symmetry of the magnetization distribution (compare Fig. 6a and Fig. 6b at the boundaries) as well. Increasing the field, one can observe an increase of: (i) the domain structure period and (ii) the volume of the domain with the magnetization oriented along H. The mean $<m_\perp(x)>$ value was drawn as a function of $H_\perp$. Changes of magnetic susceptibility can be deduced by analysis of $<m_\perp(x)>(H_\perp)$ values. The increase of susceptibility, while increasing $H_\perp$ amplitude, is connected with a decrease of the domain period.

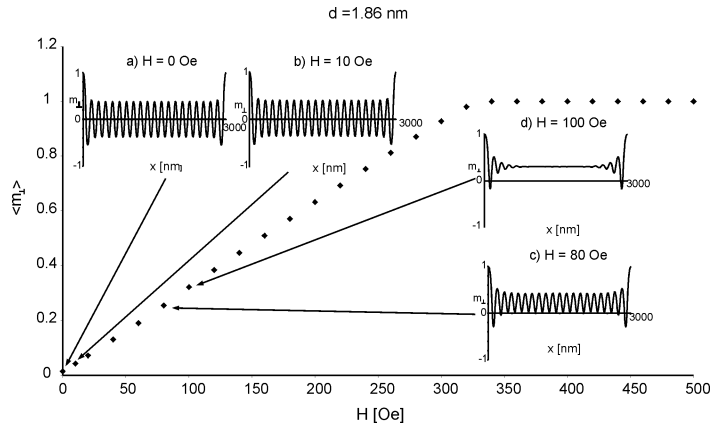

Fig. 7. Dependence of the average $<m_\perp>$ magnetization component on the external field, for d = 1.86 nm. Insets a)-d) show $m_\perp(x)$ magnetization component distributions for points indicated by arrows

An example of magnetization distribution for $d_1 < d < d^*$ is shown in Fig. 7. Inside the sample, the magnetization oscillates with an amplitude smaller than 1. The strong influence of sample wedges on the amplitude is visible. Increasing $H_\perp$ amplitude, one can find an interesting evolution of magnetization distribution inside the sample: the magnetization oscillates around a level, whose position increases, while the oscillation amplitude decreases. Vanishing of these oscillations – the "domain structure" – is visible for $H_\perp$ =100 Oe, where only sample wedges produce a magnetization in-homogeneity. Further $H_\perp$ increase induces the rotation of the magnetization in the direction of the applied field.

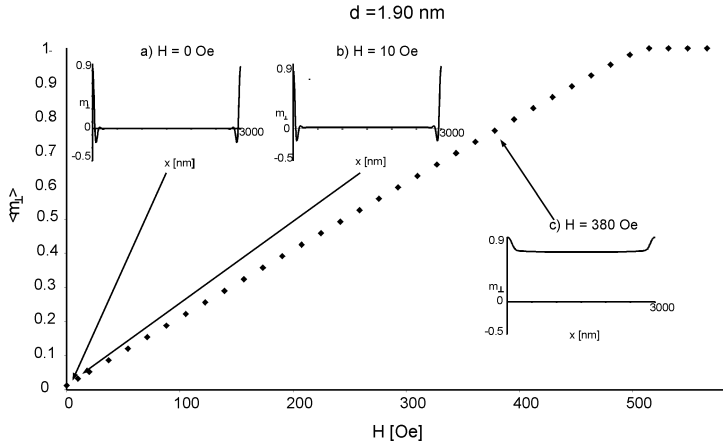

Fig. 8. Dependence of the $<m_\perp>$ magnetization component on the external field, for d = 1.90 nm. Insets a)-c) show $m_\perp(x)$ magnetization component distributions for points indicated by arrows

Figure 8 shows an example of magnetization distributions for $d > d^*$. Neglecting boundary effects, the $H_\perp$-induced magnetization process undergoes by a rotation of the magnetization from the in-plane into a perpendicular direction. This process is well described by Eq. 2, see Fig. 2.

Strong changes of magnetization distributions are presented for ultrathin film when changing magnetic anisotropy from an easy magnetization axis into an easy magnetization plane. Simulations show a sinusoidal-like distribution near the reorientation phase transition. Both the oscillation amplitude and the initial susceptibility decrease while approaching the /RPT.

References

[1] A. Hubert and R. Shäfer, *Magnetic Domains*, Springer, Berlin (1998).
[2] M. Kisielewski, A. Maziewski, T. Polyakova, and V. Zablotskii, Phys. Rev. B. **69** 184419 (2004).
[3] M. Speckman, H. P. Oepen, and H. Ibach, Phys. Rev. Lett. **75**, 2035 (1995).
[4]. M. Kisielewski A. Maziewski, M. Tekielak, A. Wawro, and T. Baczewski, Phys. Rev. Lett. **89** (2002)
[5] 087203 M. Donahue, D. Porter, Object Oriented Micromagnetic Framework, http://math.nist.gov/oommf, free software for micromagnetic simulations.
[6] M. Kisielewski, A. Maziewski, V. Zablotskii, T. Polyakova, J. M. Garcia, A. Wawro, and T. Baczewski, J. Appl. Phys. **93**, 10, 6966 (2003).
[7] M. Kisielewski, A. Maziewski, T. Polyakova, and V. Zablotskii, J. Magn. Magn. Mater. **272-276**, e825 (2004).